



University
of Glasgow

Deng, Q., Xu, J., Guo, L., Liang, S., Hou, L., and Zhu, H. (2016) A dual-grating InGaAsP/InP DFB laser integrated with an SOA for THz generation. *IEEE Photonics Technology Letters*, 28(21), pp. 2307-2310.

There may be differences between this version and the published version. You are advised to consult the publisher's version if you wish to cite from it.

<http://eprints.gla.ac.uk/130126/>

Deposited on: 17 November 2016

Enlighten – Research publications by members of the University of Glasgow
<http://eprints.gla.ac.uk>

A dual-grating InGaAsP/InP DFB laser integrated with a SOA for THz generation

Qiufang Deng, Junjie Xu, Lu Guo, Song Liang, Lianping Hou, Hongliang zhu

Abstract—We report a dual-mode semiconductor laser which has two gratings with different periods below and above the active layer. A semiconductor optical amplifier (SOA), which is integrated with the dual-mode laser, plays an important role in balancing the optical power and reducing the linewidths of the emission modes. A stable two mode emission with a 13.92 nm spacing can be obtained over a wide range of DFB and SOA injection currents. Compared with other types of dual-mode lasers, our device has the advantages of simple structure, compact size and low fabrication cost.

Index Terms—Dual-grating, THz, power balance

I. INTRODUCTION

Terahertz (THz) signal, because of its unique properties, has numerous applications such as THz imaging for quantitative analysis of industrial products [1], detection of remote explosive materials [2], as well as THz communications [3]. As a result, the generation of terahertz radiation has been drawing a lot of interests. One effective technique to generate CW THz signal is optical heterodyning of two wavelengths on a photomixer, outputting a frequency corresponding to the wavelength spacing of the two optical waves. Up to now, several kinds of light sources have been proposed for this application, such as combining the output from two discrete single frequency distributed feedback (DFB) semiconductor lasers [4], [5], multi-section DFB dual mode semiconductor laser (DML) [6]–[9] and dual-wavelength distributed Bragg reflector (DBR) lasers [7], [8]. One section DMLs with simultaneous two longitude modes emission within a single laser cavity have also been reported [10], [11]. This kind of DML is very attractive because of their compactness, stability and spectral quality. The separation between the two modes are less than several microns. The fluctuation of frequency difference between the two longitudinal modes can be reduced by the common-mode noise rejection effect [12], because the two modes are affected by the same current, thermal energy and mechanical fluctuations. Comparatively, in the multi-section DFB lasers

for photomixing such as reported in reference [6], the two modes are produced separately in two cavities which are connected in series and are driven by different currents. Thus better stability and spectral quality of devices having our structure can be expected. However, in the reported one section DMLs [10], [11], two gratings with different periods are formed on each side of the ridge waveguide to achieve the two emission wavelengths. Because the waveguide is only several microns in width, e-beam lithography facility is needed for fabricating the gratings, which is known as being not suitable for mass production of optoelectronic devices.

Here we report a DML which has two gratings with different periods below and above the active layer. A semiconductor optical amplifier (SOA), which is integrated with the dual-mode laser, plays an important role in balancing the optical power and phase-locking of the two emission modes. A stable 1.7 THz beating signal is obtained over a wide range of DFB and SOA injection currents. Compared with the multi-section DMLs as reported in [6], our device is more simple in structure and more compact in size. The optical emissions from the device reported here shows relatively narrow linewidth, which is desired for generating THz radiation. What is more, unlike previous single section DMLs, our device can be fabricated by conventional lithographic lithography, helping to lower the fabrication cost.

II. DEVICE STRUCTURE AND FABRICATION PROCEDURE

The schematic structure of the DML is shown in Fig.1 (a). The device is based on InGaAsP/InP material grown by metal organic vapor phase epitaxy (MOVPE). After the bottom grating is formed in the InP substrate in the DFB section of the device by conventional holographic exposure and dry etching, the active layer is grown, which includes a lower InGaAsP ($\lambda_{\text{PL}} = 1.2 \mu\text{m}$, where PL stands for photoluminescence) separate confinement heterostructure (SCH), multi-quantum wells (MQWs) consisting of six compressively strained InGaAsP wells ($+1.1 \times 10^{-2}$, $\lambda_{\text{PL}} = 1.52 \mu\text{m}$) and seven tensile strained InGaAsP barriers (-3×10^{-3} , $\lambda_{\text{PL}} = 1.2 \mu\text{m}$), and an upper InGaAsP SCH layer. The thickness of the well and the barrier of the MQWs are 10 nm and 5 nm, respectively. The thickness of the SCH layer is 100 nm. The PL spectrum of the active layer is shown in Fig. 1 (b), which peaks at about 1518 nm. Then, in the DFB region of the device, the upper grating of the dual-wavelength laser is formed in the upper SCH layer by a

This work was supported in part by the NSF of China under Grant 61320106013, Grant 61474112, Grant 61321063, and Grant 61274071, and in part by the National 863 Program of China under Grant 2013AA014502.

Qiufang Deng, Junjie Xu, Lu Guo, Song Liang and Hongliang Zhu are with Key Laboratory of Semiconductor Materials Science, Beijing Key Laboratory of Low Dimensional Semiconductor Materials and Devices, Institute of Semiconductors, Chinese Academy of Sciences, Beijing, 100083, China (e-mail: liangsong@semi.ac.cn, zhuhl@semi.ac.cn).

Lianping Hou is with School of Engineering, University of Glasgow, Glasgow G12 8LT, UK.

second holographic exposure and dry etching process. The periods of the gratings are 240 nm (Λ_1) for the lower grating and 242 nm (Λ_2) for the upper grating, which correspond to Bragg wavelengths of 1536 nm (λ_1) and 1548.8 nm (λ_2), respectively, considering an effective index of 3.2. Fig. 1 (c) and Fig. 1 (d) show the scanning electron microscope (SEM) images of the bottom grating and the upper grating, respectively. Finally, a p-InP cladding layer and a p+-InGaAs contact layer are grown, finishing the material growth process. A 3 μ m ridge waveguide structure is adopted for the device. The lengths of DFB section and the SOA section are 430 μ m and 40 μ m, respectively. A 30 μ m isolation section between the DFB and SOA sections is formed by removing the InGaAs contact layer.

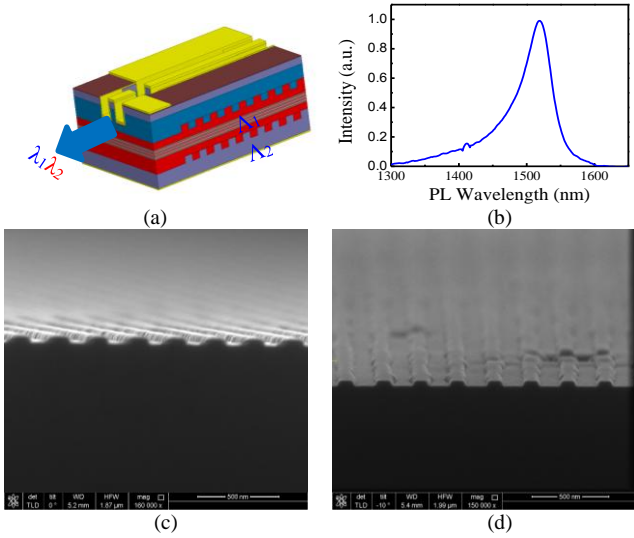


Fig. 1. (a) Schematic structure of the device, (b) PL spectra of the active layer, (c), (d) are the SEM pictures of the bottom and the upper gratings, respectively.

III. DEVICE CHARACTERIZATIONS

The DFB facet and the SOA facet of the device are high-reflection(HR) coated (90%) and anti-reflection (AR) coated (<0.05%), respectively. The device is sintered on a Cu heat sink, whose temperature is set as 20 $^{\circ}$ C during the whole test process.

A. Power performance

Fig. 2 shows the light output power from the SOA facet versus injection current (L-I) curves of the devices. When the SOA is floated, the threshold current of the laser is about 75 mA and the optical power is 20 mW with a 250 mA DFB inject current (I_{DFB}). The large threshold can be attributed mainly to the deviation of the DFB wavelengths from the PL peak of the MQWs as will be shown below. Then, the optical properties of the MQWs can be improved by optimizing the growth conditions carefully. The threshold decreases and the optical power of the laser increases with the SOA current (I_{SOA}) before I_{SOA} is smaller than 20 mA. As I_{SOA} increases to 30 mA, the output power falls because of self-heating effect and saturation of the SOA. As can be seen from the figure, there are kinks in the L-I curves. As will be shown in the following,

the operation of the device changes from dual mode to single mode emission when the kinks occur.

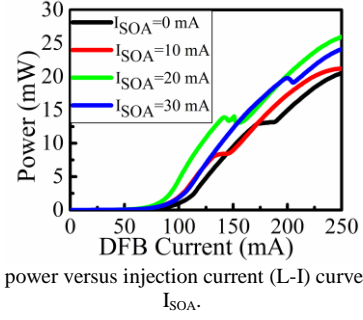


Fig. 2. Light power versus injection current (L-I) curves at different I_{SOA} .

B. Dual-mode characteristics

Fig. 3 shows the optical spectra of the device when different currents are injected into the DFB section of the device and $I_{SOA} = 0$ mA. The spectra are measured with a resolution bandwidth (RBW) of 0.01 nm. When the current is lower than 110 mA, laser operation occurs on only the shorter wavelength corresponding to the lower grating, whose Bragg wavelength is closer to the gain peak of the MQWs. As I_{DFB} is larger than 110 mA, the laser emission has two longitudinal modes with a 13.92 nm spacing. The two wavelengths are about 20nm and 30nm, respectively, longer than the peak of the PL spectrum as shown in Fig. 1. While the intensity of the shorter mode decreases with I_{DFB} , that of the longer mode increases relatively. The power variations of the two modes

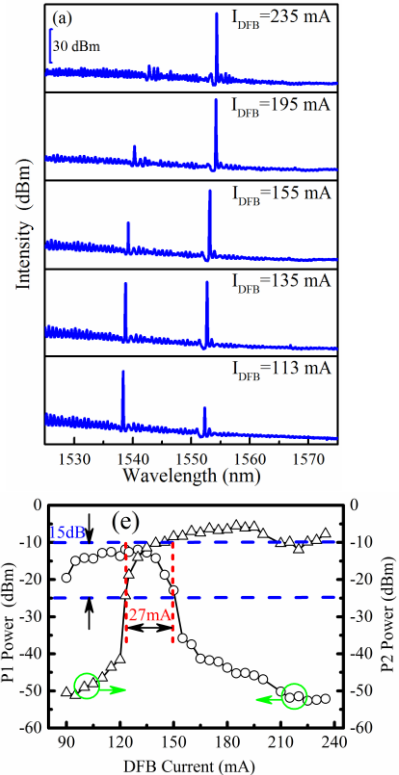


Fig. 3. Optical spectra of the device at different I_{DFB} (a), power variations of the two modes as a function of I_{DFB} when $I_{SOA}=0$ mA.

as a function of I_{DFB} when SOA is floated are shown in Fig. 3(b). The kink in the L-I curve at about 170 mA I_{DFB} as shown

in Fig. 2 corresponds to the change from dual mode to single mode operation (power difference larger than 30 dB), which might be attributed to the self-saturation and cross-saturation effects of the two mode lasing system [13], [14].

For the generation of THz signal by mixing two wavelengths, a balance power between the two wavelengths is required to obtain a high conversion efficiency between optical power and THz power. To get a smaller than 3 dB intensity difference between the two modes, I_{DFB} is needed to be in the range from 130 mA to 138 mA when $I_{SOA} = 0$ mA. As the SOA is forward biased, this range can be extended greatly. As shown in Fig. 3(a), when $I_{DFB} = 113$ mA and $I_{SOA} = 0$ mA, the intensity of the shorter wavelength is over 30 dB larger than that of the longer one. When $I_{SOA}=25.9$ mA, the intensity of the longer wavelength is increased significantly, reducing the difference to be less than 1dB as shown in Fig. 4(a). When $I_{DFB} = 235$ mA, the intensity difference can be reduced from over 40 dB as shown in Fig. 3(a) to about 1 dB with a 38.5 mA SOA current. The obtained optical spectrum is shown in Fig. 4(b). Some other working points with less than 3 dB power difference are listed in Table 1 and the detailed optical spectra are shown in Fig.5. In general, a higher I_{DFB} needs a larger I_{SOA} to ensure a small power difference between the two modes. Because the two modes are in the same cavity, they are affected by the same power, thermal energy and mechanical fluctuations, leading to simultaneous variation of the two wavelengths. The frequency difference, that is, the frequency of the THz emission can thus be stabilized effectively. The autocorrelation trace corresponding to Fig. 4(a) is shown in Fig. 4(c), which indicates a sinusoidal modulation. The average period is 588 fs, which corresponds to a 1.7 THz repetition frequency and agrees with the 13.92 nm wavelength difference of the two main modes.

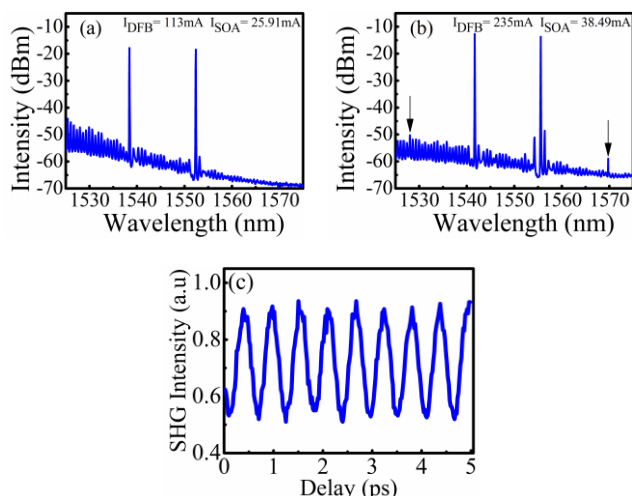


Fig. 4. Optical spectra of the device when (a) $I_{DFB} = 113$ mA , $I_{SOA} = 25.9$ mA, (b) $I_{DFB} = 235$ mA , $I_{SOA} = 38.5$ mA; (c) the measured autocorrelation pulse train corresponding to (a).

TABLE I
SOME WORKING POINTS WITH LESS THAN 3 DB POWER DIFFERENCE BETWEEN THE TWO MODES (MA)

I_{DFB}	I_{SOA}	I_{DFB}	I_{SOA}
113.0	25.9	175.0	30.7
115.0	24.6	180.0	34.1
120.0	23.7	185.0	31.1
125.0	24.3	190.0	34.1
130.0	24.7	195.0	34.1
135.0	26.3	200.0	34.1
140.0	26.8	205.0	34.8
145.0	26.9	210.0	35.8
150.0	27.1	215.0	36.0
155.0	27.9	220.0	36.3
160.0	27.9	225.0	37.1
165.0	27.7	230.0	37.6
170.0	29.9	235.0	38.5

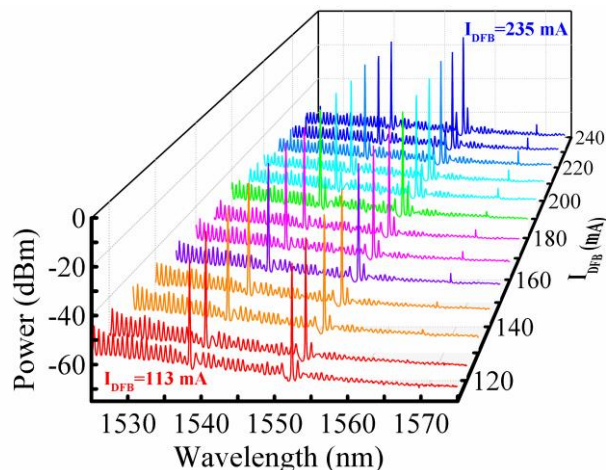


Fig.5 Optical spectra of the device when I_{SOA} is changed as shown table 1

C. Optical linewidth

The spectrum linewidth of the generated THz signal is directly related to the optical linewidths of the optical wavelengths. The optical linewidths of the modes of our laser are measured using a self-heterodyne system [15]. The measurement setup of the system is shown in Fig. 6 (a). An isolator is used to reduce the influence of light reflection. An acoustic-optic modulator (AOM) with a 70 MHz frequency shift is used in one arm. A single mode fiber (SMF) with a length of 25 km, which corresponds to a minimum measurable linewidth of 48 kHz, is used as a delay line. A photodetector (PD) detects the beat signals before the electrical spectrum analyzer (Agilent PXA-N9030A). With the help of an optical filter, the linewidth of each one of the two modes can be measured. A typical linewidth measurement result when $I_{SOA}=25$ mA is shown in Figure 6(b). When $I_{DFB} = 140$ mA, the measured linewidth as a function of I_{SOA} is shown in Figure 6(c). The linewidth increases from 1.45 MHz to 3.14 MHz as I_{SOA} increases from 0 to 17 mA. Further increase of I_{SOA} to 25 mA and 30 mA decreases the linewidth rapidly to 1.0 and 0.7 MHz, respectively. These linewidths are notably narrower than the linewidth of a conventional single grating DFB laser, which is typically over 3 MHz. In the SOA, four wave mixing (FWM) process takes place in some bias conditions. The FWM side bands at 1527.74 nm and 1569.5 nm can be clearly

seen in Fig. 4 (b) and Fig. 5. FWM has been shown to be able to reduce the linewidth by phase locking the two modes in the device reported in ref [11]. We propose that FWM also leads to the narrow linewidths of our device.

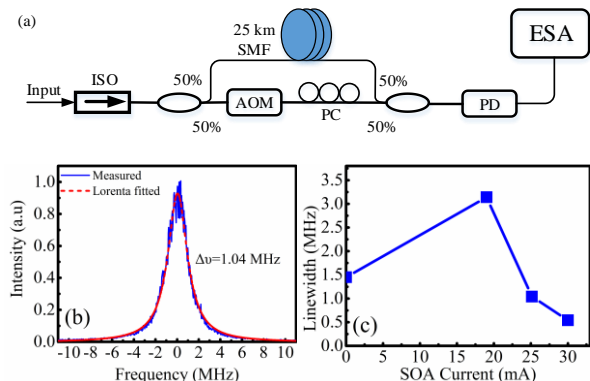


Fig. 6. (a) Schematic diagram of the linewidth measurement setup. ISO: isolator; SMF: single mode fiber; VOA: variable optical attenuator; PC: polarization controller; AOM: acoustic optical modulator; PD: photodetector; ESA: electrical spectrum analyzer; (b) Measured linewidth of the laser as a function of I_{SOA} when $I_{\text{DFB}} = 140$ mA; (c) a typical linewidth measurement result when $I_{\text{DFB}} = 140$ mA and $I_{\text{SOA}} = 25$ mA;

IV. SUMMARY

In summary, a dual-mode semiconductor laser which has two gratings with different periods below and above the active layer is reported. A SOA is integrated monolithically with the dual-mode laser and plays an important role in balancing the optical power and reducing the linewidth of the emission modes. A stable two mode emission can be obtained over a wide range of operation conditions. The device is a promising light source for THz signal generation by photomixing. The laser can be fabricated by conventional holographic lithography, helping to lower the fabrication cost.

REFERENCES

- [1] C. J. Strachan, P. F. Taday, D. A. Newnham, K. C. Gordon, J. A. Zeitler, M. Pepper, and T. Rades, "Using terahertz pulsed spectroscopy to quantify pharmaceutical polymorphism and crystallinity," *J. Pharm. Sci.*, vol. 94, no. 4, pp. 837–846, 2005.
- [2] J. F. Federici, D. Gary, B. Schulkin, F. Huang, H. Altan, R. Barat, and D. Zimdars, "Terahertz imaging using an interferometric array," *Appl. Phys. Lett.*, vol. 83, no. 12, pp. 2477–2479, 2003.
- [3] T. Kleine-Ostmann and T. Nagatsuma, "A review on terahertz communications research," *Journal of Infrared, Millimeter, and Terahertz Waves*, vol. 32, no. 2, pp. 143–171, 2011.
- [4] S. Matsuura, M. Tani, and K. Sakai, "Generation of coherent terahertz radiation by photomixing in dipole photoconductive antennas," *Appl. Phys. Lett.*, vol. 70, no. 5, p. 559, 1997.
- [5] I. S. Gregory, W. R. Tribe, C. Baker, B. E. Cole, M. J. Evans, L. Spencer, M. Pepper, and M. Missous, "Continuous-wave terahertz system with a 60 dB dynamic range," *Appl. Phys. Lett.*, vol. 86, no. 20, pp. 1–3, 2005.
- [6] N. Kim, J. Shin, E. Sim, C. W. Lee, D. Yee, M. Y. Jeon, Y. Jang, and K. H. Park, "Monolithic dual-mode distributed feedback

semiconductor laser for tunable continuous-wave terahertz generation," *Opt. Express*, vol. 17, no. 16, p. 13851, Aug. 2009.

- [7] S. D. Roh, R. B. Swint, A. M. Jones, T. S. Yeoh, A. E. Huber, J. S. Hughes, and J. J. Coleman, "Dual-wavelength asymmetric cladding InGaAs-GaAs ridge waveguide distributed Bragg reflector lasers," *IEEE Photonics Technol. Lett.*, vol. 11, no. 1, pp. 15–17, Jan. 1999.
- [8] S. D. Roh, T. S. Yeoh, R. B. Swint, A. E. Huber, C. Y. Woo, J. S. Hughes, and J. J. Coleman, "Dual-wavelength InGaAs-GaAs ridge waveguide distributed Bragg reflector lasers with tunable mode separation," *IEEE Photonics Technol. Lett.*, vol. 12, no. 10, pp. 1307–1309, Oct. 2000.
- [9] N. Kim, S.-P. Han, H.-C. Ryu, H. Ko, J.-W. Park, D. Lee, M. Y. Jeon, and K. H. Park, "Distributed feedback laser diode integrated with distributed Bragg reflector for continuous-wave terahertz generation," *Opt. Express*, vol. 20, no. 16, p. 17496, Jul. 2012.
- [10] F. Pozzi, R. M. De La Rue, and M. Sorel, "Dual-Wavelength InAlGaAs-InP Laterally Coupled Distributed Feedback Laser," *IEEE Photonics Technol. Lett.*, vol. 18, no. 24, pp. 2563–2565, Dec. 2006.
- [11] L. Hou, M. Haji, I. Eddie, H. Zhu, and J. H. Marsh, "Laterally coupled dual-grating distributed feedback lasers for generating mode-beat terahertz signals," *Opt. Lett.*, vol. 40, no. 2, p. 182, 2015.
- [12] M. Tani, O. Morikawa, S. Matsuura, and M. Hangyo, "Generation of terahertz radiation by photomixing with dual- and multiple-mode lasers," *Semicond. Sci. Technol.*, vol. 20, no. 7, pp. S151–S163, Jul. 2005.
- [13] H. Kawaguchi, "Bistable laser diodes and their applications: state of the art," *IEEE J. Sel. Top. Quantum Electron.*, vol. 3, no. 5, pp. 1254–1270, 1997.
- [14] C. F. Lin and P. C. Ku, "Analysis of stability in two-mode laser systems," *IEEE J. Quantum Electron.*, vol. 32, no. 8, pp. 1377–1382, 1996.
- [15] T. Okoshi, K. Kikuchi, and A. Nakayama, "Novel method for high resolution measurement of laser output spectrum," *Electron. Lett.*, vol. 16, no. 16, p. 630, 1980.